3rd EUROPEAN CONFERENCE ON
EARTHQUAKE ENGINEERING & SEISMOLOGY
BUCHAREST, ROMANIA, 2022

# The efficiency of seismic plus energy retrofitting to prevent the masonry infill walls out-of-plane collapse

**André Furtado** – CONSTRUCT-LESE, Faculdade de Engenharia da Universidade do Porto, Portugal, email: afurtado@fe.up.pt

**Hugo Rodrigues** – RISCO, Universidade de Aveiro, Portugal, e-mail: hrodrigues@ua.pt

**José Melo** – CONSTRUCT-LESE, Faculdade de Engenharia da Universidade do Porto, Portugal, email: josemelo@fe.up.pt

**António Arêde** – CONSTRUCT-LESE, Faculdade de Engenharia da Universidade do Porto, Portugal, email: aarede@fe.up.pt

**Humberto Varum** – CONSTRUCT-LESE, Faculdade de Engenharia da Universidade do Porto, Portugal, email: hvarum@fe.up.pt

**Abstract:** The buildings are responsible for 40% of the energy consumption and 38% of $CO_2$ emissions in the European Union, mainly because of the late implementation of the first energy codes. Around 40% of its buildings are also located in seismic prone regions and were designed with sub-standard safety requirements. It is estimated that 65% of these buildings simultaneously need energy and seismic retrofit. Recent earthquakes have demonstrated the vulnerability of the masonry infill walls against the out-of-plane seismic loadings. Several collapses were observed and caused multiple fatalities and considerable material and economic losses. This research work aims to propose and validate seismic plus energy retrofitting techniques for masonry infill walls. Four full-scale specimens were tested with different retrofitting configurations. The tests consisted of applying a semi-cyclic (loading-unloading-reloading) history of imposed displacements in the out-of-plane direction through a uniformly distributed load. The mechanical properties of the adopted materials are characterized and presented. The results will be presented in terms of out-of-plane force-displacement responses and, damage evolution. In the end, the tests' results are compared to each other to assess the effectiveness of the seismic plus energy retrofitting technique.

**Keywords:** seismic plus energy retrofitting, masonry infill walls, out-of-plane, experimental testing

## 1. Introduction

The buildings are responsible for 40% of the energy consumption and 38% of CO2 emissions in the EU, mainly because of the late implementation of the first energy codes. Around 40% of its buildings are also located in seismic prone regions and were designed with sub-standard safety requirements. It is estimated that 65% of these buildings need both energy and seismic retrofit. Specifically, in Portugal, the reinforced concrete (RC) buildings comprise about 60% of its building stock and host approximately 65% of its population. Half of these buildings were not designed according to modern seismic codes, and 70% were not designed according to any energy code (Gevorgian *et al.* 2021). Also, 20% of the Portuguese citizens are not financially able to warm their homes (Matos *et al.* 2022). There is a tremendous socio-economic and environmental need to properly upgrade the existing building stock to face and solve the citizens "energy poverty".

Recent earthquakes demonstrated the medium/high vulnerability of RC buildings not designed according to modern seismic codes. In particular, the envelopes of RC buildings were responsible for severe structural damages and collapses, casualties, and economic losses (Varum *et al.* 2017). The impact of the envelopes in post-earthquake rehabilitation costs is estimated to be about 50% of the total building repair costs (De Risi *et al.* 2019). Independent seismic (Furtado *et al.* 2020) and energy retrofitting techniques (Jelle 2011) are available for the envelopes of RC buildings. However, the validation of effective combined Seismic plus Energy (SpE) retrofitting techniques for envelopes is still missing.

Based on this motivation, this research work aims to validate the efficiency of SpE retrofitting to improve the capacity of masonry infill walls when subjected to out-of-plane (OOP) seismic loadings. For this, four full-scale specimens were tested with different retrofitting configurations, namely: one non-retrofitted (reference); one with seismic retrofitting; one with energy retrofitting and one with SpE retrofitting. The tests consisted of applying a semi-cyclic (loading-unloading-reloading) history of imposed displacements in the out-of-plane direction through a uniformly distributed load. The results will be presented in terms of OOP (i.e. out-of-plane) force-displacement responses and, damage evolution. In the end, the tests' results are compared to each other to assess the effectiveness of the seismic plus energy retrofitting technique.

## 2. Experimental campaign

### 2.1. Specimens' description

The infill wall specimens' geometric dimensions were defined as 4.20x2.30m (length and width respectively, which are representative of those existing in the Portuguese building stock according to the study developed by Furtado *et al.* (2016), and shown in Fig. 1a and Fig. 1b. The columns' and beams' cross sections were considered as 0.30x0.30m and 0.30x0.50m, respectively. Fig. 1 shows the schematic layout of the RC frame geometry with the corresponding columns' and beams' dimensions and reinforcement detailing (Fig. 1c, Fig. 1d, and Fig. 1e, respectively).

All the infill panels have equal geometry with the above mentioned in-elevation dimensions, made of hollow clay horizontal brick units with 150mm thickness, as usually found in the envelopes of RC buildings. No reinforcement was used to connect the infill panel and the surrounding RC frame, and no gaps were adopted between the panel and the frame. All the panels were built aligned with the outer side of the RC beam. Concerning the remaining materials, it was selected a M5 class mortar for the walls' construction and a concrete class C20/25 and reinforcement steel class A500 for the frame construction.

Four masonry infill walls were tested with different retrofitting strategies:

- Specimen REF – wall without retrofitting and with 1cm plaster;
- Specimen S – wall retrofitted with textile-reinforced mortar;
- Specimen E – wall retrofitted with external thermal insulation composite system;
- Specimen SpE – wall retrofitted with a merge between the external thermal insulation composite system with the textile-reinforced mortar.

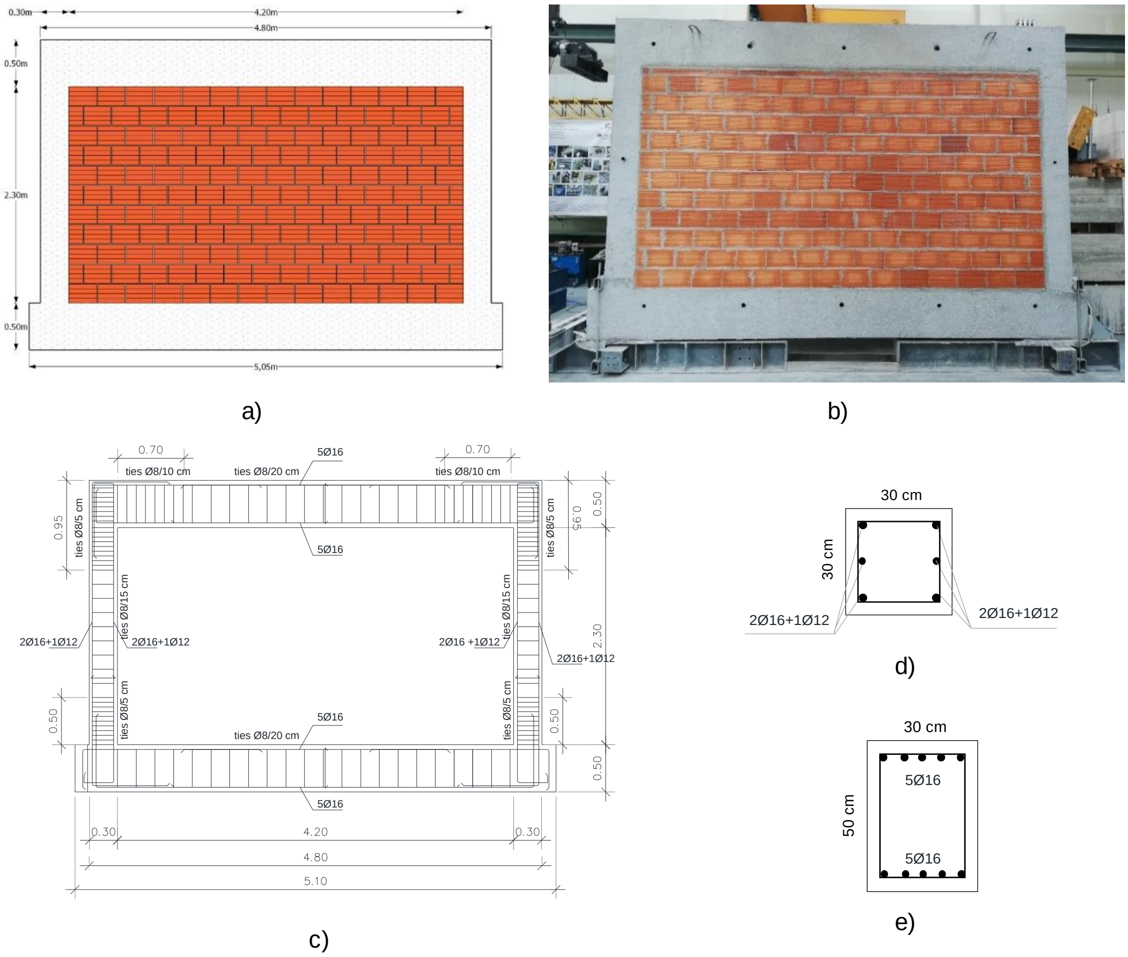


Fig. 1 – Infilled RC frame specimen dimensions (units in meters): a) general dimensions; b) front view of the specimen; c) RC frame reinforcement detailing; d) column and e) beam dimensions and reinforcement detailing

## 2.2. Description of the retrofitting strategies

The specimen "S" was retrofitted with textile-reinforced mortar technique, using a glass-fiber reinforced mesh with a tensile strength equal to 40kN/m, a ultimate strain of 3.4% and a grid equal to 16.7x16.7mm$^2$. The application procedure of this strengthening strategy started with the application of 1 cm plaster. Then plastic connectors were applied throughout the infill panel to position and fix the reinforcing mesh. The plastic connectors have been used for the tested specimens to place and fix the mesh. The roll of mesh was provided with 1 m width and 50 meters length. Five vertical strips (1 m width) were used to strengthen the wall overlapped to each other. The application of vertical strips resulted easier with respect to the application of horizontal strips (whose length can also be very different depending on the bay length). The overlap length used between each vertical strip was 10 cm. The mesh was extended for 15 cm both on the beams and columns. Then, in the overlapping regions for the transition RC frame-infill panel, a duplicated mesh was assumed with an overlap equal to 30 cm (15 cm for the RC frame and 15 cm for the infill panel). The layout of the mesh application is shown in Fig. 2a. Concerning the mesh connection to the envelope RC frame, a steel plate (3mm thick and 30mm width) was used along the perimeter of the wall (10cm from the external face of the RC element). Ø10mm holes were drilled in each location defined for the anchor to insert M8 steel connectors, as shown in Fig2b. Thus, the mesh was placed between the frame and the steel plate, which was anchored with the steel connectors to the frame. The main goal was to minimize the mesh's local sliding/shear failure. Plastic connectors were used to connect the mesh to the wall.

Specimen E was retrofitted with an external thermal insulation composite system. Again, only the exterior surface of the wall was retrofitted. First, a 1cm layer of traditional mortar (M5 class) was applied to the wall surface. Then, expanded polystyrene (EPS) plates 6cm thick, with graphite additives with thermal conductivity of 0.031 W/(m.K), were positioned and fixed using an adhesive mortar. Also, the positioning of the EPS plates was performed using plastic connectors to connect them to the wall and the RC frame, as shown in Fig. 2c. According to the supplier's recommendations, four plastic connectors per square meter were adopted per square meter. After that, a new thin layer of adhesive mortar (around 0.5mm) was applied to fix a non-structural mesh that aims to prevent cracking due to temperature variations, as shown in Fig. 2d. Finally, the retrofitting was concluded with the application of 1cm plaster.

Specimen SpE was retrofitted with a SpE technique, which consisted of applying the external thermal insulation composite system and the textile-reinforced mortar. The retrofitting started by fixing the EPS plate, used in wall E, using an adhesive layer. After that, it was applied over the external surface of the EPS plate a new layer of adhesive mortar (0.5cm), as shown in Fig. 2e. The GFRP mesh applied in the wall S was applied in the front of the EPS layer, using the same layout (i.e. overlapping frame-wall, between mesh stripes) as shown in Fig. 2f. The GFRP mesh was connected to the wall and the frame using plastic bushing with steel screws. The geometric distribution of these connectors was the same adopted in wall S. After that, a new layer of adhesive plaster was applied to the wall surface to receive the non-structural mesh to prevent cracking. The retrofitting was concluded with the application of 1 cm plaster.

a)

b)

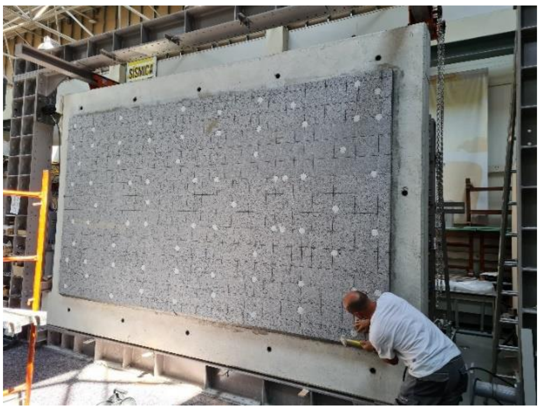

c)

d)

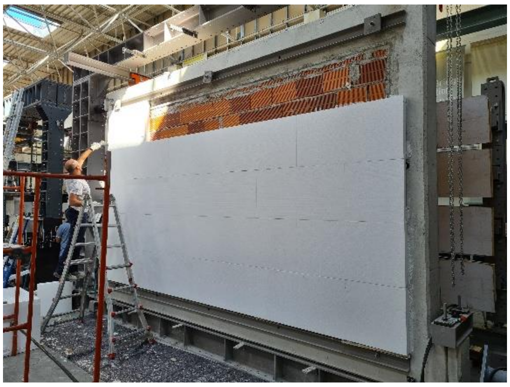
e)


f)

Fig. 2 – Specimens' retrofitting: a) General view of wall S; b) Detail of the mesh-frame connection; c) Detail of the positioning of the EPS plates; d) Detail of the application of the non-structural mesh; e) detail of the EPS application and e) layout of the structural mesh application.

## 2.3. Test setup

The experimental test consisted of applying a uniform OOP load applied by 28 pneumatic actuators, which are linked to a self-equilibrated reaction steel structure composed of four horizontal alignments made with HEB140 steel profiles and five vertical alignments made with HEB220 steel profiles (Fig. 3). The vertical alignments are hinged, allowing their rotation during the tests. The steel reaction structure is attached to the envelope frame in twelve points (five in each top and bottom beam and one in each column). In each of these connections, a load cell was placed that allowed to monitor the loads during the tests.

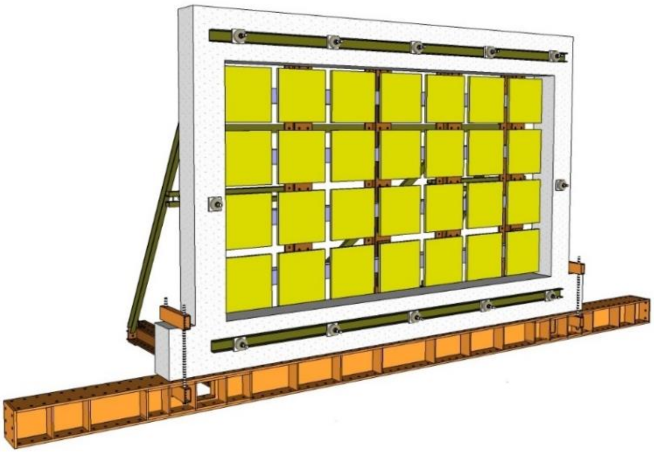
a)


b)

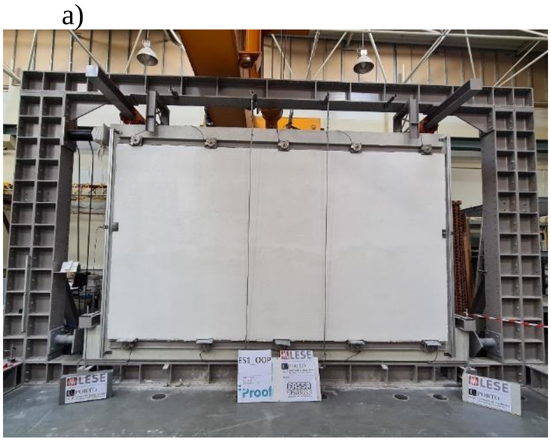
c)

Fig. 3 – Test setup: a) schematic layout; b) lateral view; and c) front view.

The instrumentation was composed of 21 displacement transducers, thirteen of them related to monitoring the panel OOP displacements and the remaining eight to the rotation between the panel and the envelope frame. Apart from that, and as explained in the previous subsection, twelve load cells were used to monitor the loadings developed during the test. The pressure level inside the pneumatic actuators was set by two pressure valves which were controlled according to the target and measured OOP displacement of the central point of the infill panel (the control node and variable) continuously acquired during the tests using a data acquisition and control system developed in the National Instruments LabVIEW software platform (Vicente *et al*. 2012).

Two half-cyclic (loading-unloading) OOP displacements were imposed with steadily increasing displacement levels, targeting the following nominal peak displacements: 0.5; 1;2.5; 5; 7.5; 10; 15; 20; 25; 30; 35; 40; 45; 50; 50; 55; 60; 65, 70, 75, 80, 85, 90, 95 and 100mm. The central geometric point of the panel was selected as the control point since it was expected that is the region where it will occur the largest deformation of the panel.

## 3. Test results and discussion

### 3.1. Specimen Ref

During the testing of the reference specimen, it was not observed damage until the OOP displacement equal to 5mm. At this level of OOP displacement occurred the plaster detachment in some parts of the panel. After that, at the OOP displacement equal to 7.5mm, the beginning of a horizontal cracking was observed at 1/3 of the panel height. When the panel reached the OOP displacement equal to 15mm, the horizontal crack became more pronounced and, at the same time appeared a vertical crack at the middle of the panel, from the top until the horizontal crack. When the OOP displacement reached 25mm diagonal cracks were visible, which started in the same alignment of the horizontal crack until the bottom of the panel. At the end, at the OOP displacement equal to 30mm, the panel collapsed. The cracking pattern was essentially trilinear, as evidenced in Fig. 4a. Fig. 4b presents the force-displacement response curve, from which it is possible to observe that for the OOP displacement equal to 2mm occurred the first decrease of strength, which was quickly recover and followed by a progressive increase until the 6mm (instant where it was visible the beginning of plaster detachment). After that, a progressive increase of the OOP strength can be verified until a maximum peak load equal to 61.2kN occurred for an OOP displacement equal to 29mm. After that, at the OOP displacement equal to 29.8mm, the panel suddenly collapsed without any visible previous decrease of the OOP strength.


a)

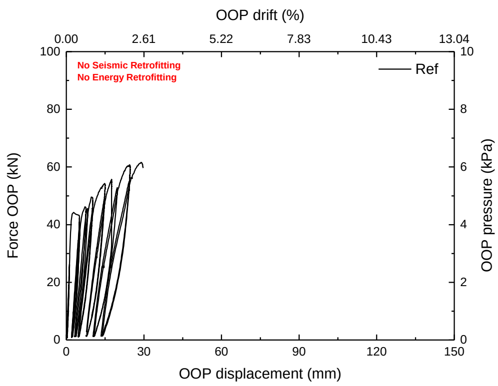


b)

Fig. 4 – Specimen Ref: a) Cracking pattern; and b) Force-displacement curve.

### 3.2. Specimen S

The first macro-cracking occurred for an OOP drift equal to 0.17% and was a horizontal crack above the mid-height panel. Again, diagonal and horizontal cracks appear until the maximum peak load (92.31kN) corresponding to a drift of 2.55%. After that, it occurred the fracture/crushing of the bricks located at the firs and, consequently, the OOP strength reduced about 44kN and the OOP drift suddenly increased until approximately 7%.
Until the last stage of the test, it was not observed any significant reduction of the panel strength and the residual capacity of the panel was found equal to 42.61kN for an OOP drift equal to 8.70%. The test has stopped due to the limit of the pneumatic actuators stroke. The panel cracking pattern is shown in Fig 5a. The mesh-frame anchorage in the top and bottom of the wall was found in good conditions, which was vital to prevent the wall collapse.

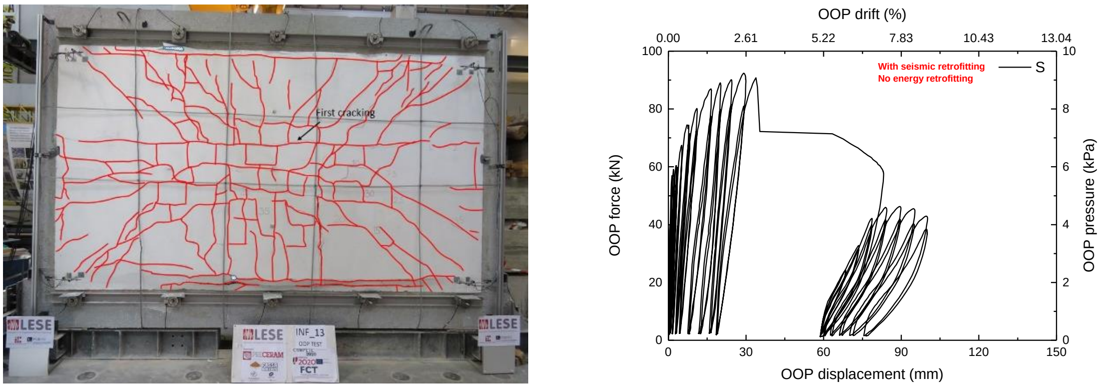


a) b)

Fig. 5 – Specimen S: a) Cracking pattern; and b) Force-displacement curve.

### 3.3. Specimen E

During the testing of the specimen E, it was not observed any cracking over the wall surface. Even for large OOP displacements, the non-structural mesh prevented the cracking. It was observed a rigid body behaviour during the whole test. A first OOP strength drop was observed for an OOP displacement equal to 9.62mm caused by the detachment of the wall from the top beam. After that, an increase of the OOP strength was observed due to the arching mechanism, but without any cracking development, which is a novelty in this type of testing. The maximum strength of 55.8kN was reached for an OOP displacement of 60mm. After that, the collapse of the wall occurred suddenly, resulting from the total detachment of the wall from the top interface, as shown in Fig. 6a. The force-displacement curve is plotted in Fig. 6b.

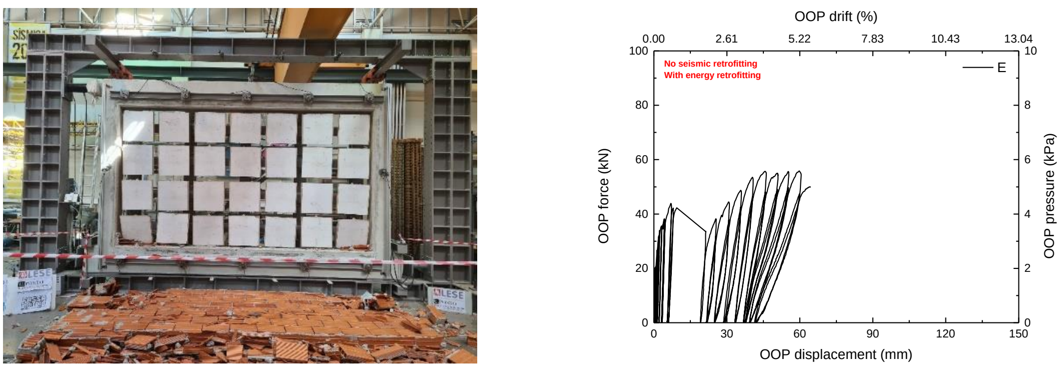


a) b)

Fig. 6 – Specimen E: a) Collapse of the wall; and b) Force-displacement curve.

### 3.4. Specimen SpE

During the testing of specimen SpE, it was once again noticed that it was not observed any cracking development, even for large OOP displacements. A continuous increase of the OOP force was observed until 4.7mm when a slight detachment of the panel from the top beam interface was noticed. Therefore, the maximum strength of 81.35kN was reached for an OOP displacement of 22.9mm. The total detachment between the wall and the top and bottom RC beams was observed at this stage. Then, the OOP strength was reduced until the wall collapsed for the OOP displacement of 132mm. From the test, it becomes pretty clear the efficiency of the retrofitting and the excellent performance of the anchorage system of the retrofitting material to the RC frame. Even for large OOP displacements, the connection adopted to fix the retrofitting material performed well, without fragile rupture.

a)

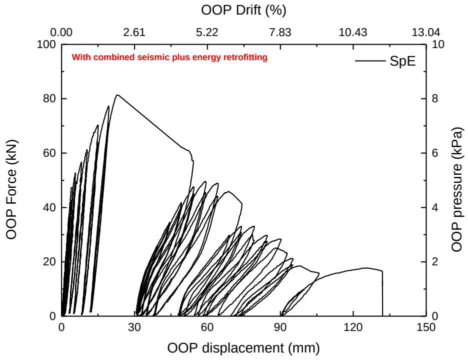


b)

Fig. 7 – Specimen E: a) Collapse of the wall; and b) Force-displacement curve.

### 3.5. Global comparison

From the global overview of the test results, the SpE retrofitting technique was quite efficient in strength and displacement capacity. In terms of OOP strength the SpE specimen reached a maximum OOP load of only 11% lower than the one reached by the wall with seismic retrofitting (i.e. specimen S). Concerning the comparison between the walls Ref and E, it was observed that the wall with SpE retrofitting reached an OOP strength 33% and 46% higher than them.

Concerning the displacement capacity, the SpE retrofitting prevented the wall collapse until large deformation demands. In contrast, the walls Ref and E collapsed for low to medium displacement demands, proving the high vulnerability of these typologies of walls.

## 4. Conclusions

Recent earthquakes evidenced that the infill panels are vulnerable to OOP loadings, which could result in serious human and economic consequences. Also, the buildings are responsible for a significant part of the energy consumption and CO2 emissions because most of the existing buildings were not designed according to any energy codes. They need energy retrofitting to improve their energy efficiency.

Based on this motivation, this research work aims to validate the efficiency of SpE retrofitting to improve the capacity of masonry infill walls when subjected to out-of-plane (OOP) seismic loadings. For this, four full-scale specimens were tested with different retrofitting configurations, namely: one non-retrofitted (reference); one with seismic retrofitting; one with energy retrofitting and one with SpE retrofitting. The tests consisted of applying a semi-cyclic (loading-unloading-reloading) history of imposed displacements in the out-of-plane direction through a uniformly distributed load. The results showed that the SpE retrofitting performance was very interesting by increasing the OOP strength and deformation capacity 32% and 342% higher than the reference specimen. The fragile collapse was prevented. Future tests will be carried out to assess the efficiency of similar solutions to combined in-plane and OOP loadings.

## Acknowledgements

This work was financially supported by: Base Funding - UIDB/04708/2020 and Programmatic Funding - UIDP/04708/2020 of the CONSTRUCT - Instituto de I&D em Estruturas e Construções - funded by national funds through the FCT/MCTES (PIDDAC). This work was also supported by the Foundation for Science and Technology (FCT) - Aveiro Research Centre for Risks and Sustainability in Construction (RISCO), Universidade de Aveiro, Portugal [FCT/UIDB/ECI/04450/2020].

COMPETE 2020 PORTUGAL 2020 UNIÃO EUROPEIA Fundo Europeu de Desenvolvimento Regional FCT Fundação para a Ciência e a Tecnologia MINISTÉRIO DA CIÊNCIA, TECNOLOGIA E ENSINO SUPERIOR

The authors would also like to acknowledge the Laboratory of Earthquake and Structural Engineering (LESE) technicians: Mr. Guilherme Nogueira and Mr. Nuno Pinto, for their support in the experimental activity reported in this research work.

## References

De Risi, M. T., C. Del Gaudio and G. M. Verderame (2019). "Evaluation of repair costs for masonry infills in RC buildings from observed damage data: The case-study of the 2009 L'Aquila earthquake." Buildings **9**(5).

Furtado, A., C. Costa, A. Arêde and H. Rodrigues (2016). "Geometric characterisation of Portuguese RC buildings with masonry infill walls." European Journal of Environmental and Civil Engineering: pp. 1-16.

Furtado, A., H. Rodrigues, A. Arêde and H. Varum (2020). "Experimental tests on strengthening strategies for masonry infill walls: A literature review." Construction and Building Materials **263**.

Gevorgian, A., S. Pezzutto, S. Zambotti, S. Croce, U. Oberegger, R. Lollini, L. Kranzl and A. Müller (2021). European Building Stock Analysis: A country by country descriptive and comparative analysis of the energy performance of buildings.

Jelle, B. (2011). "Traditional, state-of-the-art and future thermal building insultation materials and solutions-properties, requirements and possibilities." Energy and Buildings **43**: 2549-2563.

Matos, A., J. M. P. Q. Delgado and A. S. Guimarães (2022). "Linking Energy Poverty with Thermal Building Regulations and Energy Efficiency Policies in Portugal." Energies **15**(1): 329.

Varum, H., A. Furtado, H. Rodrigues, J. Dias-Oliveira, N. Vila-Pouca and A. Arêde (2017). "Seismic performance of the infill masonry walls and ambient vibration tests after the Ghorka 2015, Nepal earthquake." Bulletin of Earthquake Engineering **15**(3): 1185-1212.

Vicente, R., H. Rodrigues, H. Varum, A. Costa and R. Mendes da Silva (2012). "Performance of masonry enclosure walls: lessons learned from recent earthquakes." Earthquake Engineering and Engineering Vibration **11**(1): 23-34.